J Membrane Biol (2013) 246:915–926
DOI 10.1007/s00232-013-9593-0

Relative CO_2/NH_3 Permeabilities of Human RhAG, RhBG and RhCG

R. Ryan Geyer · Mark D. Parker · Ashley M. Toye · Walter F. Boron · Raif Musa-Aziz

Received: 11 April 2013 / Accepted: 5 September 2013 / Published online: 29 September 2013

Abstract Mammalian glycosylated rhesus (Rh) proteins include the erythroid RhAG and the nonerythroid RhBG and RhCG. RhBG and RhCG are expressed in multiple tissues, including hepatocytes and the collecting duct (CD) of the kidney. Here, we expressed human RhAG, RhBG and RhCG in *Xenopus* oocytes (vs. H_2O-injected control oocytes) and used microelectrodes to monitor the maximum transient change in surface pH (ΔpH_S) caused by exposing the same oocyte to 5 % CO_2/33 mM HCO_3^- (an increase) or 0.5 mM NH_3/NH_4^+ (a decrease). Subtracting the respective values for day-matched, H_2O-injected control oocytes yielded channel-specific values (*). $(\Delta pH_S^*)_{CO_2}$ and $(-\Delta pH_S^*)_{NH_3}$ were each significantly >0 for all channels, indicating that RhBG and RhCG—like RhAG—can carry CO_2 and NH_3. We also investigated the role of a conserved aspartate residue, which was reported to inhibit NH_3 transport. However, surface biotinylation experiments indicate the mutants $RhBG_{D178N}$ and $RhCG_{D177N}$ have at most a very low abundance in the oocyte plasma membrane. We demonstrate for the first time that RhBG and RhCG—like RhAG—have significant CO_2 permeability, and we confirm that RhAG, RhBG and RhCG all have significant NH_3 permeability. However, as evidenced by $(\Delta pH_S^*)_{CO_2}/(-\Delta pH_S^*)_{NH_3}$ values, we could not distinguish among the CO_2/NH_3 permeability ratios for RhAG, RhBG and RhCG. Finally, we propose a mechanism whereby RhBG and RhCG contribute to acid secretion in the CD by enhancing the transport of not only NH_3 but also CO_2 across the membranes of CD cells.

Keywords Gas channel · Rhesus protein · Biotinylation · Surface pH · Collecting duct

R. R. Geyer · M. D. Parker · W. F. Boron · R. Musa-Aziz
Department of Physiology and Biophysics, Case Western Reserve University School of Medicine, Cleveland, OH 44106, USA

A. M. Toye
School of Biochemistry, University of Bristol, Medical Science Building, Bristol, UK

R. Musa-Aziz (✉)
Department of Physiology and Biophysics, University of São Paulo, Av Prof Lineu Prestes 1524, São Paulo 05508-000, Brazil
e-mail: raifaziz@icb.usp.br

Introduction

The regulation of blood pH within the normal range (7.35–7.45) is one of the most important physiological processes because the structure and function of virtually all proteins are directly influenced by pH.

With a person on a typical Western diet, cellular metabolism produces ~40 mmol of net H^+/day (Giebisch and Windhager 2009). In addition, the transfer of dietary H^+ from the gastrointestinal tract to the extracellular fluid, as well as the obligatory loss of alkali in stool, represents a net gain of an additional 30 mmol of H^+/day (Giebisch and Windhager 2009). The total daily H^+ load of ~70 mmol titrates ~70 mmol of HCO_3^- from body fluids to produce CO_2 (which the lungs excrete) and H_2O. If the HCO_3^- consumed in this buffer reaction were not constantly replenished, a catastrophic metabolic acidosis would ensue. To maintain plasma [HCO_3^-] and thus pH, the kidney—operating in a steady state—must perform three related tasks: (1) reabsorb the ~4,000 mmol/day of HCO_3^- filtered in the glomeruli (this operation merely prevents the loss of HCO_3^- into the urine), (2) transfer to the blood plasma an additional ~70 mmol/day of "new" HCO_3^- to

replenish the HCO_3^- lost to H^+ buffering and (3) secrete into the tubule lumen ~70 mmol/day of H^+ that is produced during the process of generating the "new" HCO_3^-. Virtually all of the secreted H^+ titrates buffers that increase the H^+-carrying capacity of the tubule fluid.

The most important of these urinary buffers is NH_3/NH_4^+, nearly all of which is synthesized de novo by the proximal tubule (PT). Deamidation of glutamine to glutamate and then α-ketoglutarate in the PT mitochondria yields two molecules of NH_4^+. Metabolism of α-ketoglutarate generates two HCO_3^- ions, which exit the cell across the basolateral membrane via the Na/HCO_3^- cotransporter (NBCe1-A) (Boron and Boulpaep 1983; Romero et al. 1997) for entry into the blood. The newly formed NH_4^+ dissociates in the PT cell to form NH_3 and H^+. The NH_3 exits across the apical membrane of the cell—probably at least in part via AQP1 (Nakhoul et al. 2001; Musa-Aziz et al. 2009a)—entering the tubule lumen. There, the NH_3 reacts with H^+—secreted mainly via the Na–H exchanger NHE3 (Nagami 1988)—to reform NH_4^+. The medullary thick ascending limb (mTAL) reabsorbs much of the NH_4^+, which—as considered in "Discussion"—eventually enters the lumen of the collecting duct (CD) in a complex series of events.

From the above discussion, it is clear that the net movement of NH_3/NH_4^+ from the TAL lumen to the CD lumen is critical. Four lines of evidence suggest that the rhesus (Rh) glycoproteins RhBG and RhCG make a substantial contribution to the movement of NH_3 across the membranes of the CD cells:

(1) In heterologous expression systems RhBG and RhCG both transport NH_3 (Bakouh et al. 2006; Mak et al. 2006; Weiner and Verlander 2010).
(2) In the kidney RhBG and RhCG are expressed mainly in the CD α-intercalated cells (Eladari et al. 2002; Quentin et al. 2003; Verlander et al. 2003; Seshadri et al. 2006; Biver et al. 2008; Brown et al. 2009), far more so than in principal cells (Seshadri et al. 2006). RhBG is expressed only in the basolateral membrane (Quentin et al. 2003; Verlander et al. 2003; Han et al. 2006; Kim et al. 2009), whereas RhCG is expressed in both the basolateral membranes (Han et al. 2006; Seshadri et al. 2006; Brown et al. 2009; Kim et al. 2009) and apical membranes (Eladari et al. 2002; Quentin et al. 2003; Verlander et al. 2003; Han et al. 2006; Seshadri et al. 2006; Biver et al. 2008; Brown et al. 2009; Kim et al. 2009).
(3) In response to chronic metabolic acidosis, wild-type (WT) mice increase RhBG (Bishop et al. 2010) and RhCG (Seshadri et al. 2006) protein abundance, consistent with a role in the support of acid excretion.
(4) When subjected to chronic metabolic acidosis, mice with intercalated-cell–specific knockouts of RhBG (Bishop et al. 2010) or RhCG (Lee et al. 2010) transiently excrete less urinary NH_3/NH_4^+ than WT mice.

Previous work shows that the Rh glycoprotein related to RhBG and RhCG—namely, RhAG—transports not only NH_3 (Ripoche et al. 2006; Musa-Aziz et al. 2009a) but also CO_2 (Endeward et al. 2008; Musa-Aziz et al. 2009a). Moreover, when compared to the bacterial Rh protein AmtB and various mammalian aquaporins (AQPs), RhAG exhibits a characteristic selectivity for NH_3 versus CO_2 (Musa-Aziz et al. 2009a; Geyer et al. 2013b). Thus, important questions are whether RhBG and RhCG also conduct CO_2 and, if so, how the CO_2/NH_3 selectivities of RhBG and RhCG compare to those of AQPs and other Rh proteins. In the present study we expressed RhBG, RhCG or, as a control, RhAG in *Xenopus* oocytes and used microelectrodes to monitor the transient changes in cell-surface pH (pH_S) as we exposed cells to CO_2 or NH_3. The maximal excursions of pH_S (ΔpH_S) are semiquantitative indices of CO_2 and NH_3 permeability. We found that both RhBG and RhCG conduct CO_2 and NH_3. However, the CO_2/NH_3 permeability ratios for RhAG, RhBG and RhCG were indistinguishable from one another. Based on our results, we propose a model whereby basolateral RhBG and RhCG enhance the uptake not only of NH_3 (Mak et al. 2006; Kim et al. 2009; Wagner et al. 2009; Gruswitz et al. 2010) but also of CO_2 across the basolateral membranes of CD cells. This CO_2 uptake would be anticipated to promote basolateral Cl-HCO_3^- exchange and thus help drive H^+ secretion into the CD lumen.

Materials and Methods

Expression in *Xenopus* Oocytes

cDNA Clones

RhAG and the *Xenopus* expression vector BSXG have been described previously (Bruce et al. 2009). BSXG-RhBG and RhCG were generated from pGFPC1-RhBG and pGFPC1-RhCG constructs (Brown et al. 2009) by double restriction digest, using *Bgl*II and *Xma*I and ligated into a *Bgl*II and *Xma*I precut BSXG4 vector. The site-directed mutants $RhBG_{D178N}$ and $RhCG_{D177N}$ were generated using the QuikChange Site-Directed Mutagenesis Kit (catalog 200518; Stratagene, Cedar Creek, TX) according to the manufacturer's protocol. The sequence of all clones was confirmed by DNA sequencing (Eurofin MWG Operon,

London, UK; Keck DNA Sequencing Facility, New Haven, CT).

cRNA Synthesis

The restriction enzyme *Xho*I was used to linearize the pBSXG plasmid containing human RhBG, $RhBG_{D178N}$, RhCG or $RhCG_{D177N}$ cDNA. Linearized cDNAs were then purified using the QIAquick PCR purification kit (Qiagen, Valencia, CA). Transcribed, capped cRNA was generated using the T7 mMessage mMachine kit (Ambion, Austin, TX); and these cRNAs were purified and concentrated using the RNeasy MinElute RNA Cleanup Kit (Qiagen).

Xenopus Oocyte Isolation

Oocytes were isolated from female *Xenopus laevis* frogs according to methods described previously (Musa-Aziz et al. 2010). Briefly, we surgically removed ovaries from frogs anesthetized in 0.2 % MS-222 (ethyl 3-aminobenzoate methanesulfonate; Sigma-Aldrich, St. Louis, MO). The ovarian lobes were dissected into small pieces and washed in 0-Ca solution (in mM: 98 NaCl, 2 KCl, 1 $MgCl_2$, 5 HEPES [pH 7.5], osmolality 195 mOsm/kg) prior to enzymatic defolliculation with 2 mg/ml type IA collagenase (Sigma-Aldrich) in 0-Ca. Stage V–VI oocytes were selected and stored at 18 °C in filter-sterilized OR3 medium that contained (per 2 l) one pack of powdered Leibovitz L-15 medium (13.7 g/pack) with L-glutamine (GIBCO-BRL, Grand Island, NY), 100 ml of 10,000 U/ml penicillin, 10,000 U/ml streptomycin solution (Sigma-Aldrich) and 5 mM HEPES titrated to pH 7.5, osmolality ~195 mOsm/kg H_2O until use.

Microinjection of cRNAs

One day after isolation, oocytes were injected with either 25 ng of cRNA encoding human RhBG, $RhBG_{D178N}$, RhCG or $RhCG_{D177N}$ cRNA (delivered as 25 nl of a 1 ng/nl cRNA solution) or 25 nl of sterile water (Ambion) for control, H_2O-injected oocytes. After injection, we stored oocytes at 18 °C in OR3 medium for 4–5 days before using them in experiments.

Protein Expression Measurements

Biotinylation

Biotinylation of plasma membrane–resident proteins was performed using the EZ-Link Sulfo-NHS-Biotinylation Kit (part no. 21425; Thermo Fisher Scientific, Rockford, IL) according to the manufacturer's recommendations, with some previously described modifications (Geyer et al. 2013a, b). Briefly, groups of 30 oocytes were incubated with Sulfo-NHS-Biotin biotinylation reagent at 4 °C × 1 H. The biotinylation reaction was terminated by adding the supplied quenching buffer and washing the cells in TBS. Cells were lysed by trituration in lysis buffer (TBS that contained 1 % Triton X-100 and a cOmplete EDTA-free protease inhibitor tablet; part no. 11873580001; Roche, Indianapolis, IN). The insoluble fraction was pelleted by centrifugation, and a sample of the supernatant containing solubilized protein ("total protein" fraction) was set aside for Western-blot analysis. Biotinylated protein was isolated from the remainder of the solubilized fraction by incubation at room temperature for 1 h with immobilized NeutrAvidin gel (Invitrogen, Carlsbad, CA). Nonbiotinylated protein was rinsed from the gel by repeated washing with lysis buffer. Biotinylated protein was subsequently eluted from the gel using 300 µl of 1× SDS sample buffer (Invitrogen) containing 50 mM DTT ("biotinylated protein" fraction).

Western-blot Analysis

Total and biotinylated protein samples were separated by SDS-PAGE on 12 % Tris–glycine gels (Invitrogen). Samples were transferred to PVDF membranes using the iBlot apparatus (Invitrogen) for 8 min. Membranes were rinsed with TBST (Tris-buffered saline/Tween, in mM: 50 Tris-base, 150 NaCl [pH 7.4], 0.1 % Tween 20 [#P7949, Sigma-Aldrich]) and then transferred to TBST plus 5 % powdered milk. Membranes were probed with one of a number of rabbit primary C-terminal polyclonal antibodies raised against human RhAG (Toye et al. 2008), RhBG or RhCG (Brown et al. 2009), followed by a goat anti-rabbit secondary monoclonal antibody (AP132P; Millipore, Billerica, MA), and detected using ECL plus Western Blotting Detection Reagents (GE Healthcare Life Sciences, Pittsburgh, PA).

Electrophysiological Measurements

Chamber

Oocytes were placed in plastic perfusion chamber, with a channel 3 mm wide × 30 mm long; saline constantly flowed down this channel at a rate of 4 ml/min. Perfusing solutions were delivered using syringe pumps (Harvard Apparatus, South Natick, MA). Switching between solutions was performed by pneumatically operated valves (Clippard Instrument Laboratory, Cincinnati, OH). All experiments were performed at room temperature (~22 °C).

Transport Assay Solutions

The ND96 solution contained (in mM) 96 NaCl, 2 KCl, 1 $MgCl_2$, 1.8 $CaCl_2$ and 5 HEPES (pH 7.50), with osmolality

195 mOsm. The CO_2/HCO_3^- solution was identical to ND96 except that 33 mM $NaHCO_3$ replaced 33 mM NaCl and the solution was bubbled with 5 % CO_2/balanced O_2. The 0.5 mM NH_3/NH_4^+ solution was made by first replacing 5 mM NaCl with 5 mM NH_3/NH_4^+ and then diluting the solution 1:10 with standard ND96 solution.

Measurement of Surface pH

Our approach for monitoring the pH_S of an oocyte has been described in detail elsewhere (Musa-Aziz et al. 2009a; Geyer et al. 2013b). We measured pH_S using a pH electrode with a tip diameter of ~15 µm, which was filled with H^+ ionophore mixture B (95293; Fluka Chemical, Ronkonkoma, NY) and amplified by an FD223 electrometer (World Precision Instruments, Sarasota, FL). The external reference electrode for the pH_S measurements was a calomel half-cell (connected to a model 750 electrometer, World Precision Instruments) contacting a 3 M KCl–filled micropipette, which contacted the fluid in the chamber. We also recorded intracellular pH (pH_i) and V_m in each experiment, as described previously (Musa-Aziz et al. 2009a, b) but do not report these data. The analog subtraction of the calomel–electrode signal from the pH_S–electrode signal produced the signal due to pH_S. We used an ultrafine micromanipulator (model MPC-200 system; Sutter Instrument, Novato, CA) to position the pH_S electrode tip at the surface of the oocyte and then to advance it ~40 µm farther, forming a slight dimple in the membrane. For routine recalibration of the electrode, we periodically withdrew the electrode from the surface of the oocyte and positioned it in the bulk extracellular fluid (BECF, pH 7.50). The tip of the pH_S microelectrode, with respect to the flow of solution, was positioned near the oocyte's equator, in the "shadow" of the oocyte.

Analysis of pH_S Data

We used an approach described previously (Endeward et al. 2006; Musa-Aziz et al. 2009a, b) to compute the maximum magnitude (i.e., "spike height" or ΔpH_S) of the pH_S transient elicited by applying a solution containing either extracellular 5 % CO_2/HCO_3^- or 0.5 mM NH_3/NH_4^+. In brief, we determined the initial pH_S—before the application of CO_2/HCO_3^- or NH_3/NH_4^+—by comparing the pH_S–electrode voltage signal when the electrode tip was at the oocyte surface with the voltage signal obtained when the tip was in BECF lacking CO_2/HCO_3^- and NH_3/NH_4^+ (7.50). We determined the maximum pH_S during exposure to CO_2/HCO_3^- and the minimum pH_S during exposure to NH_3/NH_4^+ by comparing the voltage signal (at a time corresponding to the extreme pH_S value) when the electrode tip was at the oocyte surface with the voltage signal obtained a few minutes later, when the tip was in the BECF containing CO_2/HCO_3^- or NH_3/NH_4^+ (7.50). ΔpH_S is the algebraic difference between the extreme and initial pH values. All oocytes used in this study had initial V_m values at least as negative as −40 mV.

In Vitro Assay of Carbonic Anhydrase Activity

To determine carbonic anhydrase (CA) activity, we used a colorimetric assay—conducted at 0 °C—to monitor a fall in pH (Brion et al. 1988; Musa-Aziz et al. 2009a). The sample mixture consisted of 10 µl of protein (20 µg) from a membrane preparation of oocytes injected with cRNA (25 ng) encoding human CA IV, RhAG, RhBG or RhCG plus 185 µl H_2O and 5 µl of 1-octanol, for a total volume of 200 µl. In some experiments, we reduced the amount of injected hCA IV to 0.25 µg. We bubbled the sample mixture with 100 % CO_2 and then added 200 µl of buffer/indicator mix (5.0 mM Tris·HCl, 20 mM imidazole and 0.4 mM para-nitrophenol, pH 8.00), thereby reducing $[CO_2]$ by half. The color of this CO_2-rich solution was initially yellow, indicating a relatively alkaline solution. A yellow-to-clear color change—due to the reaction $CO_2 + H_2O \rightarrow HCO_3^- + H^+$—indicates the reaction end point. We used a stopwatch to measure the time to achieve the end point. Protein concentrations of samples were determined using the Pierce® BCA Protein Assay Kit (Thermo Scientific).

Statistics

Data are presented as mean ± SEM. To compare the difference between two means, we performed Student's *t* tests (two-tailed). To compare more than two means, we performed a one-way ANOVA followed by a Student–Newman–Keuls post hoc analysis, using KaleidaGraph (version 4; Synergy Software, Reading, PA). $p < 0.05$ was considered significant.

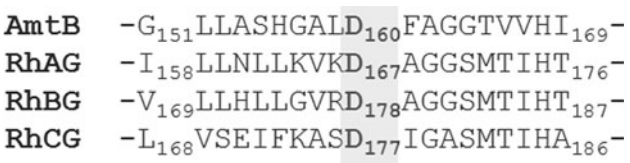

Fig. 1 Multiple sequence alignment of RhAG, RhBG and RhCG. Using CLUSTALW, a sequence alignment was generated to illustrate the conserved aspartate group in AmtB, RhAG, RhBG and RhCG. The residue D160 in AmtB (Javelle et al. 2004) and the homologous D177 in RhCG (Marini et al. 2006) have been reported to be critical for NH_3 transport. This residue is also conserved in RhAG and RhBG. The WT sequence used for AmtB was Swissprot P69681. GenBank accession numbers for the other proteins were AF031548 (RhAG), AF193807 (RhBG) and AF193809 (RhCG)

Results

Our goal was to use pH_S measurements to determine whether—like RhAG—RhBG and RhCG are permeable to both CO_2 and NH_3. We examined not only the WT proteins but also constructs in which we mutated a highly conserved Asp residue to Asn (Fig. 1).

pH_S Transients Induced by CO_2 Entry

Oocytes Injected with H_2O

When we added CO_2/HCO_3^- to BECF, if the influx of CO_2 dominated over the entry of HCO_3^- in terms of pH_S changes, the entry of CO_2 into the cell created a deficit of CO_2 near the outer surface of the membrane (Fig. 2a, left side). CO_2 diffusion from BECF partially replenished the deficit. However, additional replenishment occurred via the following reactions at the outer surface of the cell: $HCO_3^- + H^+ \rightarrow H_2CO_3 \rightarrow H_2O + CO_2$. The result was the consumption of protons and thus a rapid rise, or "spike," in pH_S that decayed exponentially from its peak toward pH_{Bulk} as the CO_2 influx gradually slowed. The light gray record on the left side of Fig. 2b shows the pH_S trajectory for a H_2O-inected oocyte (replicated in Fig. 2c, d). The maximal pH_S spike height (ΔpH_S) is a semiquantitative index of the rate of CO_2 entry. Thus, other things being equal, ΔpH_S is an index of the permeability to CO_2, although the relationship between ΔpH_S and permeability is not expected to be linear (Somersalo et al. 2012).

Oocytes Expressing RhAG

The left side of Fig. 2b also shows the effect of expressing RhAG on the pH_S trajectory elicited by exposure to CO_2 (black record). As was the case with the H_2O-injected oocyte, exposure to CO_2/HCO_3^- caused a rapid rise in pH_S, followed by an exponential decay. However, the expression of RhAG increased the magnitude of ΔpH_S compared to day-matched, H_2O-injected control oocytes. Thus, RhAG increased the CO_2 permeability of the oocyte, consistent with the earlier work of Musa-Aziz et al. (2009a).

Oocytes Expressing RhBG

The left side of Fig. 2c (black record) shows that expressing RhBG produced a CO_2-induced pH_S trajectory that was similar to that observed above with RhAG. On the other hand, with an oocyte expressing $RhBG_{D178N}$ (Fig. 2c, gray record), the magnitude of ΔpH_S was only slightly greater than that of the day-matched, H_2O-injected oocyte.

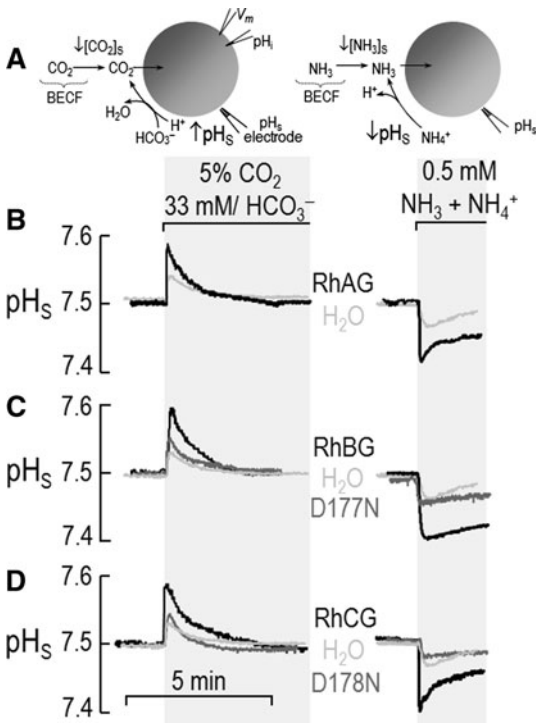

Fig. 2 Surface pH (pH_S) measurements in oocytes exposed to CO_2/HCO_3^- or NH_3/NH_4^+. **a** Cell models. **b** RhAG and H_2O. **c** RhBG, $RhBG_{D178N}$ and H_2O. **d** RhCG, $RhCG_{D177N}$ and H_2O. In each experiment, the same *oocyte* was sequentially exposed to ND96, the 5 % CO_2/33 mM HCO_3^- solution, ND96 again and then finally the 0.5 mM NH_3/NH_4^+ solution. During the exposure, pH_S measurements were recorded throughout the course of the experiment. We exposed the oocyte to CO_2/HCO_3^- for a period of time long enough for the pH_S to rise and then decay to a stable value. Then, following the washout of CO_2/HCO_3^- ($\sim$15 min, long enough for pH_i to stabilize), the same oocyte was exposed to NH_3/NH_4^+ .Routinely, we moved the electrode away from the surface of the oocyte to calibrate it in the bath solution

Oocytes Expressing RhCG

The left side of Fig. 2d (black record) shows that an oocyte expressing RhCG likewise exhibited a much greater ΔpH_S than the day-matched, H_2O-injected control. On other hand, the oocyte expressing $RhCG_{D177N}$ (gray record), like the one expressing $RhBG_{D178N}$, produced a pH_S trajectory that was indistinguishable from that of the H_2O-injected control oocyte.

pH_S Transients Induced by NH3 Entry

Oocytes Injected with H_2O

When we added NH_3/NH_4^+ to the BECF, if the entry of NH_3 dominated over the entry of NH_4^+ in terms of pH_S changes, the influx of NH_3 created a deficit in NH_3 at the outer surface of the cell membrane (Fig. 2a, right side). Diffusion of NH_3 from the BECF partially replenished the

deficit. However, the NH_3 deficit was also replenished by the following reaction at the outer surface of the cell: $NH_4^+ \rightarrow NH_3 + H^+$. This resulted in the production of protons and thus a rapid fall in pH_S that decayed toward pH_{Bulk} as the NH_3 influx gradually slowed. The light gray record on the right side of Fig. 2b (replicated in Fig. 2c, d) illustrates the pH_S trajectory for an H_2O-injected oocyte. The maximum pH_S spike depth (ΔpH_S) is a semiquantitative index of the rate of NH_3 entry. Thus, ($-\Delta pH_S$) reflects the permeability to NH_3.

Oocytes Expressing RhAG

The right side of Fig. 2b (black record) shows the effect of expressing RhAG on the ΔpH_S changes induced by exposing the cell to NH_3. As we saw with the H_2O-injected oocyte above, the NH_3/NH_4^+ exposure caused a rapid pH_S decrease and a slower decay. However, the magnitude of ΔpH_S was substantially greater for the RhAG-expressing oocyte compared to the H_2O-injected oocyte. These results confirm the results of others (Ripoche et al. 2004, 2006; Musa-Aziz et al. 2009a) that RhAG is an NH_3 channel.

Oocytes Expressing RhBG

Previous studies, using methodologies different from those presented in the present work, have demonstrated that RhBG transports NH_3 (Ludewig 2004; Zidi-Yahiaoui et al. 2005; Mak et al. 2006). The right side of Fig. 2c (black record) shows that an oocyte expressing RhBG responded to NH_3 in much the same way as an oocyte expressing RhAG, with a large $-\Delta pH_S$ indicative of NH_3 permeability. As we saw with CO_2, the oocyte expressing $RhBG_{D178N}$ had a ΔpH_S response that was very similar to that of an H_2O-injected oocyte when exposed to NH_3/NH_4^+ (Fig. 2c, gray record).

Oocytes Expressing RhCG

As for RhBG, the NH_3 permeability of RhCG has been reported (Ludewig 2004; Zidi-Yahiaoui et al. 2005; Bakouh et al. 2006; Mak et al. 2006), though using pH_i monitoring. The right side of Fig. 2d (black record) confirms that RhCG is an effective NH_3 channel. However, in the oocyte expressing $RhCG_{D177N}$, exposure to NH_3/NH_4^+ elicited a pH_S response that was very similar to that of the day-matched, H_2O-injected oocyte (Fig. 2d, gray record).

Although not shown, our recordings of V_m revealed no evidence of an electrogenic flux of NH_4^+.

Taken together, our data indicate that the WT proteins RhAG, RhBG and RhCG all transport both CO_2 and NH_3.

Analysis of Surface Expression

It has been proposed by Gruswitz et al. (2010) that these conserved Asp residues—D178N in RhBG and D177N in RhCG—serve to stabilize these Rh proteins. If the D-to-N mutations destabilize RhBG and RhCG, then it is possible that the oocyte synthesizes but rapidly degrades the mutants, fails to traffic the mutant to the plasma membrane at a normal rate or retrieves the mutant from the plasma membrane at an excessive rate. In any case, the surface abundance of the mutant proteins would be low. To investigate the extent to which the low functional expression of $RhBG_{D178N}$ and $RhCG_{D177N}$ reflects a low plasma membrane abundance, we biotinylated oocytes expressing RhAG, RhBG, $RhBG_{D178N}$, RhCG and $RhCG_{D177N}$ and performed Western blotting of both the total protein fraction and the biotinylated (i.e., plasma membrane–resident) protein fractions using previously described polyclonal C-terminal RhAG, RhBG and RhCG antibodies.

Figure 3a is a Western blot that shows the total and surface expression of RhAG. The band at $\sim$38 kDa represents the unglycosylated or core-glycosylated protein, whereas the immunoreactive higher–molecular weight pattern centered around 50 kDa is consistent with mature N-linked glycosylated protein. Based on such blots, we estimate that a substantial proportion of the total RhAG expression is resident in the plasma membrane fraction (44 ± 3 %, $n = 4$) and that most of the surface protein has a mature glycosylation (70 ± 9 %, $n = 4$).

Figure 3b is similar to Fig. 3a except that it focuses on WT RhBG and $RhBG_{D178N}$. The introduction of the D178N mutation substantially reduced total expression (in our experiments we estimated an average 68 ± 3 % reduction compared to WT, $n = 4$). Both WT and $RhBG_{D178N}$ were expressed to the plasma membrane: 43 ± 6 % ($n = 4$) of total in the case of WT and 22 ± 7 % ($n = 4$) for the mutant. An interesting observation is that virtually all of the $RhBG_{D178N}$ protein, both total and surface, was at a molecular weight consistent with unglycosylated or core-glycosylated protein.

Figure 3c is similar to Fig. 3b except that it focuses on RhCG and $RhCG_{D177N}$. We estimated that 30 ± 3 % ($n = 4$) of total WT RhCG protein was resident in the plasma membrane fraction. On the other hand, $RhCG_{D177N}$ expression was barely detectable in the total and plasma membrane fractions. Thus, although injecting oocytes with cRNA encoding WT RhBG or RhCG resulted in the robust accumulation of the cognate protein in the plasma membrane, injection of cRNA encoding the mutant $RhBG_{D178N}$ or $RhCG_{D177N}$ resulted in little protein in the plasma membrane.

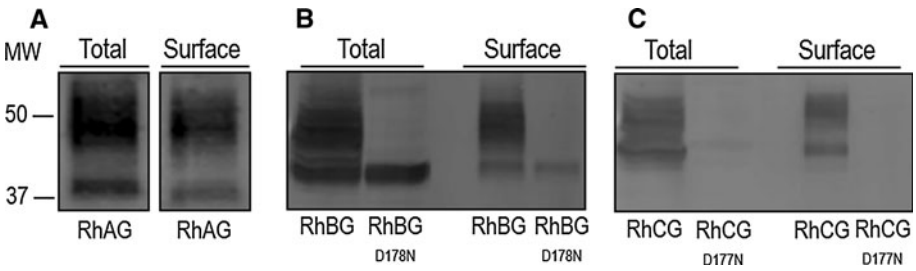

Fig. 3 Surface expression of RhAG, RhBG, $RhBG_{D178N}$, RhCG and $RhCG_{D177N}$. We assessed the total and surface expression of RhAG, RhBG, RhBG, $RhBG_{D177N}$, RhCG and $RhCG_{D178N}$ by biotinylating 30 intact oocytes injected with cRNA for each protein channel and used anti-RhAG, anti-RhBG or anti-RhCG to detect protein abundance. **a** RhAG. We detected the protein in both the total and surface fractions. There was also a characteristic high-molecular weight pattern consistent with mature *N*-linked glycosylation in both samples. **b** RhBG. We also detected glycosylated WT RhBG in both total and surface fractions. However, the abundance of $RhBG_{D178N}$ in the total fraction was greatly reduced and lacked any detectable glycoslyation. The abundance of the mutant protein was also greatly reduced at the cell surface. **c** RhCG. We detected WT protein in the total and surface fractions but were unable to detect appreciable amounts of $RhCG_{D177N}$ in either fraction. Molecular weight (MW) markers are displayed to the left

Summary of ΔpH_S Data

Figure 4 summarizes the ΔpH_S data for a larger number of experiments like those in Fig. 2b–d. Here, we ignored the two mutants, which were not appreciably present at the plasma membrane. We paired each oocyte expressing a WT channel with its day-matched, H_2O-injected control. Figure 4a shows that application of CO_2/HCO_3^- yields to a mean ΔpH_S for RhAG, RhBG or RhCG that is significantly greater than that for day-matched, H_2O-injected controls.

Figure 4b shows that the mean ΔpH_S produced by the application of NH_3/NH_4^+ for RhAG, RhBG or RhCG is significantly greater than that for day-matched, H_2O-injected controls. These observations demonstrate that RhBG and RhCG—like RhAG—function not only as NH_3 channels but also as CO_2 channels.

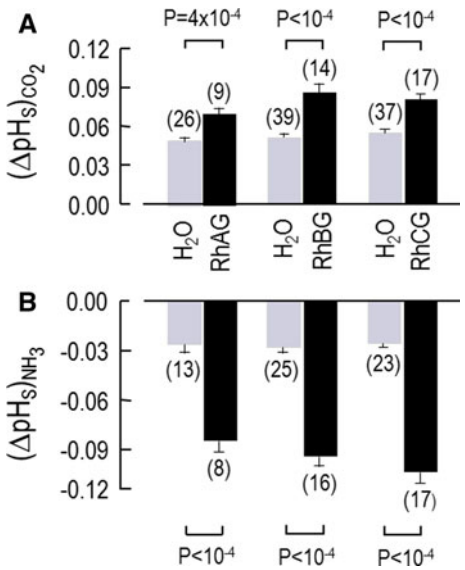

Fig. 4 Data summary for the ΔpH_S measurements. The bars summarize the results of a larger number of experiments, like those shown in Fig. 2. **a** Maximum pH_S excursions evoked by CO_2 exposure. Upon exposure to a flowing solution of 5 % CO_2/33 mM HCO_3^-, H_2O-injected control oocytes became more alkaline. However, in the oocytes expressing RhAG, RhBG or RhCG, the alkalinization—as shown by a larger $(\Delta pH_S)_{CO_2}$, value—was greater than that of H_2O-injected oocytes. **b** Maximum pH_S excursions evoked by NH_3 exposure. When the same oocyte was exposed to 0.5 mM NH_3/NH_4^+, the magnitude of the acidification $(\Delta pH_S)_{NH_3}$ in the RhAG-, RhBG- or RhCG-expressing oocytes was also greater than in H_2O-injected control oocytes. For $RhBG_{D178N}$ and $RhCG_{D177N}$ the $(\Delta pH_S)_{CO_2}$ and $(\Delta pH_S)_{NH_3}$ values (not shown) were not statistically different from the H_2O-injected control values. We performed Student's *t* test (two-tailed) for statistical comparisons

Channel-Dependent Gas Transport

The portion of the CO_2-induced ΔpH_S signal that we can ascribe to a particular channel is the difference between the ΔpH_S of each channel-expressing oocyte (e.g., black bars in Fig. 4a) and the mean ΔpH_S of the day-matched, H_2O-injected controls (e.g., light gray bars in Fig. 4a). Figure 5a summarizes these differences, computed oocyte by oocyte, for the CO_2 data—the channel-dependent signal $(\Delta pH_S^*)_{CO_2}$. Similarly, Fig. 5b summarizes the analogous differences for the NH_3 data—the channel-specific signal $(\Delta pH_S^*)_{NH_3}$. The six mean values—semiquantitative indices of channel-dependent gas permeability—are all significantly greater than 0. Note that the values in Fig. 5 are not true permeabilities but, rather, indices of relative CO_2 or NH_3 permeabilities, as determined by the product of intrinsic (or per channel) gas conductance and the number of channel proteins in the plasma membrane.

Ratios of Indices of Permeability—Gas Selectivity

In three previous studies, we examined the relative CO_2/NH_3 selectivities of AQPs 0–9 (Musa-Aziz et al. 2009a; Geyer et al. 2013b.), RhAG (Musa-Aziz et al. 2009a),

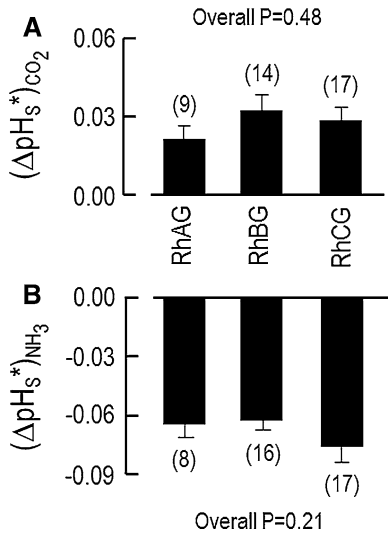

Fig. 5 Index of channel-dependent permeability to CO_2 or NH_3. **a** Channel-dependent ΔpH_S for CO_2. **b** Channel-dependent ΔpH_S for NH_3. By subtracting the $(\Delta pH_S)_{CO_2}$ or $(\Delta pH_S)_{NH_3}$ for the H_2O-injected control oocytes (see Fig. 4) from the $(\Delta pH_S)_{CO_2}$ or $(\Delta pH_S)_{NH_3}$ of RhAG-, RhBG- or RhCG-expressing oocytes (see Fig. 4), we obtained $(\Delta pH_S^*)_{CO_2}$, a semiquantitative index of channel-dependent CO_2 permeability, or $(-\Delta pH_S^*)_{NH_3}$, a semiquantitative index of channel-dependent NH_3 permeability. In all cases, the ΔpH_S values were significantly different from 0. However, the $(\Delta pH_S^*)_{CO_2}$ values were similar for RhAG, RhBG and RhCG; the same is true for the $(-\Delta pH_S^*)_{NH_3}$ values. We did not compute these values for $RhBG_{D178N}$ and $RhCG_{D177N}$, inasmuch as these proteins are not expressed at the oocyte membrane surface. We performed a one-way ANOVA to assess statistical significance

the bacterial Rh homolog AmtB (Musa-Aziz et al. 2009a) and the urea transporter UT-B (Geyer et al. 2013a). We found that each channel has a characteristic ratio $(\Delta pH_S^*)_{CO_2}/(\Delta pH_S^*)_{NH_3}$, which is a relative index of the actual CO_2/NH_3 permeability ratio. From the data that contribute to Fig. 5, we can obtain similar information about RhBG and RhCG by dividing, oocyte by oocyte, $(\Delta pH_S^*)_{CO_2}$ by the $(\Delta pH_S^*)_{NH_3}$ or, conversely, dividing $(\Delta pH_S^*)_{NH_3}$ by $(\Delta pH_S^*)_{CO_2}$. The numerical values in Fig. 6 are not ratios of true permeabilities but relative indices of CO_2/NH_3 or NH_3/CO_2 permeability ratios that we can compare from channel to channel if we obtain the data under identical experimental conditions. Our one-way ANOVA indicated no statistically significant difference among the ratios in Fig. 6.

CA Activity

In principle, the enhanced pH_S spike produced by exposing Rh-expressing oocytes to CO_2 (see left side of Fig. 2b–d and data summarized in Figs. 4a and 5a) could have been caused not by CO_2 conduction through the Rh protein but by CA activity in the Rh protein itself or an oocyte protein

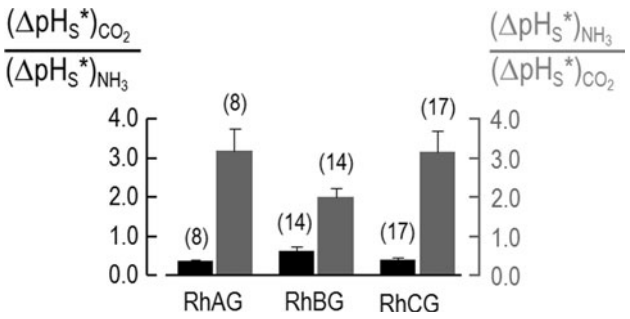

Fig. 6 Gas selectivity of RhAG, RhBG and RhCG. Using the data underlying Fig. 5, we calculated an index of relative CO_2/NH_3 permeability ratio by dividing, oocyte by oocyte, $(\Delta pH_S^*)_{CO_2}$ by $(\Delta pH_S^*)_{NH_3}$ or $(-\Delta pH_S^*)_{NH_3}$ by $(\Delta pH_S^*)_{CO_2}$

expressed in response to the Rh protein. To test the CA hypothesis, we injected oocytes with H_2O or with cRNA encoding CA IV (in which the catalytic domain was coupled via a GPI linkage to the outer surface of the membrane), RhAG, RhBG or RhCG. Previous work has shown that graded increases in the amount of injected cRNA encoding CA IV cause a graded increase in ΔpH_S (see supplemental Fig. S2 in Musa-Aziz et al. 2009a). Figure 7a shows that membrane preparations of oocytes injected with 12 ng CA IV cRNA/oocyte (we obtained similar results with 0.25 ng/oocyte; not shown), compared to H_2O oocytes, required a much shorter time to achieve the pH end point in a colorimetric CA assay. However, membrane preparations of RhAG, RhBG or RhCG oocytes are indistinguishable from those of H_2O. Figure 7b, c shows that oocytes from this preparation, when exposed to CO_2 or NH_3, exhibited pH_S changes similar to those in Fig. 5. Thus, we can rule out the hypothesis that the expression of RhAG, RhBG or RhCG increased the size of CO_2-induced pH_S changes by engendering CA activity either in the cytosol or on the surface of the oocyte.

Discussion

Overview

In the present study, we made two main observations. First, we show for the first time that RhBG and RhCG transport not only NH_3 but also CO_2 (Figs. 2, 4). Bakouh et al. (2006) performed one preliminary experiment on an H_2O-injected oocyte and one on an RhCG-expressing oocyte in which they monitored pH_i while exposing the cells to a solution containing CO_2. Their data are consistent with the hypothesis that RhCG increases the rate of CO_2-induced fall in pH_i. We are aware of no reports concerning the CO_2 permeability of RhBG. Han et al. (2009) point out that RhBG and RhCG, although present in the bronchial

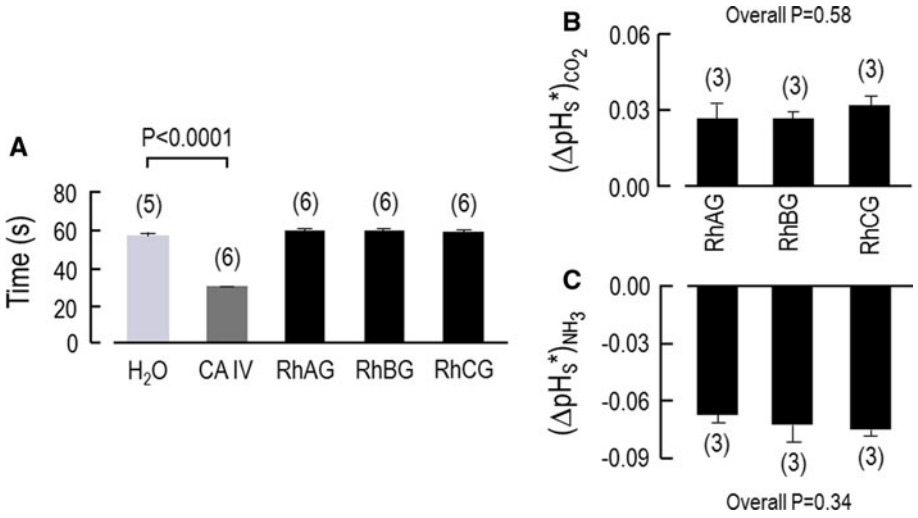

Fig. 7 Assessing the carbonic anhydrase activity of oocytes expressing Rh proteins. **a** Colorimetric assays of carbonic anhydrase (CA) activity of membrane preparations created from oocytes injected with H_2O (negative control) or 12 ng/oocyte of cRNA encoding CA IV (positive control) or 25 ng/oocyte of cRNA encoding RhAG, RhBG or RhCG. The value on the *y*-axis indicates the time necessary for the color to change. We injected 100 oocytes of each type, made a membrane preparation of each group and then repeated the colorimetric assay the indicated number of times. Other experiments (not shown) revealed that the time to the color change ($\sim$30 s) was the same after injecting either 25 ng cRNA/oocyte or 0.25 ng/oocyte. **b** Channel-dependent ΔpH_S for CO_2 addition in three oocytes from the same batch of oocytes used in **a**. **c** Channel-dependent ΔpH_S for NH_3 addition for the same three oocytes as in **b**. Values are mean $\pm$ SE, with numbers of oocytes in parentheses. For **a**, we performed Student's *t* test (two-tailed) for statistical comparisons and, for **b** and **c**, we performed one-way ANOVA, followed by Student–Newman–Keuls analyses

epithelium of the lung, are absent from alveoli and, thus, are not in a position to contribute to CO_2 transport. However, they did not examine the CO_2 permeabilities of the two Rh proteins.

Second, we find that the mutation of the conserved aspartate residues in RhBG (D178N) or RhCG (D177N) substantially reduces the abundance of the channel protein in the oocyte plasma membrane (Fig. 3). Consistent with this interpretation, we find that the mutation of RhBG results in the near-total loss of the high–molecular weight product that presumably represents mature, glycosylated RhBG. Others had proposed that these residues play a role in the deprotonation of NH_4^+ (Javelle et al. 2004; Marini et al. 2006). Our data do not allow us to address the deprotonation hypothesis, inasmuch as the surface abundance of the mutant RhBG and RhCG is so low as to preclude the detection of channel-mediated transport. Our data do support the proposal of Gruswitz et al. (2010) that the mutation of the residues would cause a structural disruption.

The RhBG cDNA used in the present study is the original human full-length clone (Lopez et al. 2005). Recently, Han et al. (2013) described a new variant of human RhBG, caused by deletion of a single cytosine base, resulting in a frame shift in which residues 425–441 (17 aa) are replaced by new residues 425–459 (35 aa). Because the N terminus and the entire transmembrane spanning domains are unaffected, we think it is likely that the permeability properties of the original and new forms of RhBG are identical. The implications of the new variant for trafficking and regulation remain to be explored.

Gas Channels

The dogma had been that all gases freely diffuse through all membranes simply by dissolving into and diffusing through the lipid phase of the membrane. However, numerous publications have challenged this view. The first evidence challenging the diffusion of gases across membranes came from the observations that apical membranes of gastric-gland cells are impermeable to CO_2 and NH_3 (Waisbren et al. 1994) and that apical membranes of colonic crypts are impermeable to NH_3 (Singh et al. 1995). The second piece of evidence challenging the dogma was the identification of the first family of gas channels, with the demonstration that AQP1, heterologously expressed in *Xenopus* oocytes, can conduct CO_2 (Nakhoul et al. 1998; Cooper and Boron 1998). In these experiments, the authors used as an index of CO_2 permeability the initial rate at which pH_i declines (dpH_i/dt). Because this dpH_i/dt approach is somewhat insensitive, Nakhoul et al. (1998) enhanced CO_2 influx by injecting CA II protein into the oocytes, whereas Cooper and Boron (1998) dissected away the vitelline membrane. Neither of these auxiliary maneuvers is necessary with the pH_S approach used in the present study. Coexpression of CA II presumably would cause the increase in ΔpH_S to the extent in the present study, limited

by the overall dynamic range of our system (solution changes, chamber, pH_S electrode).

Later work showed that AQP1 also conducts NH_3 (Nakhoul et al. 2001) and nitric oxide (Herrera et al. 2006; Herrera and Garvin 2007). The rhesus proteins became the second known family of gas channels with the demonstration that they can conduct NH_3 (Ripoche et al. 2004). Work with red blood cells (RBCs) demonstrated that the Rh complex contributes CO_2 permeability (Endeward et al. 2008). We recently described a third family of gas channels, exemplified by the urea transporter UT-B, which conducts NH_3 (Geyer et al. 2013a). Moreover, work on AQPs and rhesus proteins expressed in *Xenopus* oocytes indicates that each channel has a characteristic selectivity for CO_2 versus NH_3 (Musa-Aziz et al. 2009a; Geyer et al. 2013b).

The CO_2 permeability of plant AQPs is important for providing CO_2 for photosynthesis (Uehlein et al. 2003, 2012; Kaldenhoff and Fischer 2006; Kaldenhoff 2012), and the CO_2 permeability of AQP1 (Endeward et al. 2006) is responsible for about half of the CO_2 permeability of RBCs.

Preliminary work shows that either the injection of CA II or the expression of CA IV increases both the maximal rate of pH_i descent and the ΔpH_S spike caused by CO_2 influx (Musa-Aziz, Occhipinti, and Boron, unpublished). The CA assays summarized in Fig. 7a rule out the possibility that the enhanced CO_2-induced pH_S changes produced by RhAG, RhBG and RhCG are due to the CA activity of the rhesus proteins per se or of endogenous oocyte proteins. Previous work (Musa-Aziz et al. 2009a) led to a similar conclusion for AQP1. Thus, we can conclude that—like several AQPs—the three rhesus proteins examined in the present study act as channels for CO_2 and NH_3.

Possible Physiological Roles of RhBG and RhCG

The ability of RhBG and RhCG to conduct both CO_2 and NH_3 is reminiscent of the gas-transport properties of the related erythroid rhesus protein RhAG (Musa-Aziz et al. 2009a). In RBCs, the CO_2 permeability of RhAG could enhance the uptake of CO_2 in systemic tissues, for delivery to the lung. Similarly, the NH_3 permeability of RhAG could promote the uptake the NH_3 from systemic tissues, for delivery to the liver for detoxification.

What roles do RhBG and RhCG play in the CD in acid–base homeostasis? Others have proposed that the NH_3 permeabilities of RhBG and RhCG are critical for NH_3/NH_4^+ secretion during the defense against metabolic acidosis (Biver et al. 2008; Lee et al. 2009, 2010; Bishop et al. 2010; Gruswitz et al. 2010; Wagner et al. 2011; Weiner and Verlander 2011).

Figure 8 summarizes the handling of NH_3/NH_4^+ by the mTAL and CD. The mTAL reabsorbs NH_4^+ via apical Na/K/2Cl cotransporters (with NH_4^+ replacing K^+) and K^+ channels (Attmane-Elakeb et al. 2001). Inside the TAL cell, NH_4^+ dissociates into H^+ and NH_3. Via unknown mechanisms, the NH_3 exits across the TAL basolateral membrane and enters the interstitial fluid of the renal medulla. A portion of this NH_3 recycles back to the late PT and thin descending limb, some NH_3 enters the bloodstream for detoxification to urea in the liver and the remaining NH_3 passes through the basolateral and apical membranes of the CD cell and enters the lumen, where it is trapped as NH_4^+ and excreted in the urine. To the extent that NH_3/NH_4^+ moves from the TAL lumen to the CD lumen, it bypasses the cortical segments of the distal nephron, where—due to the permeability of the cortical nephron segments to NH_3/NH_4^+ and the greater blood flow of the cortex versus the medulla—toxic quantities of NH_3/NH_4^+ could otherwise

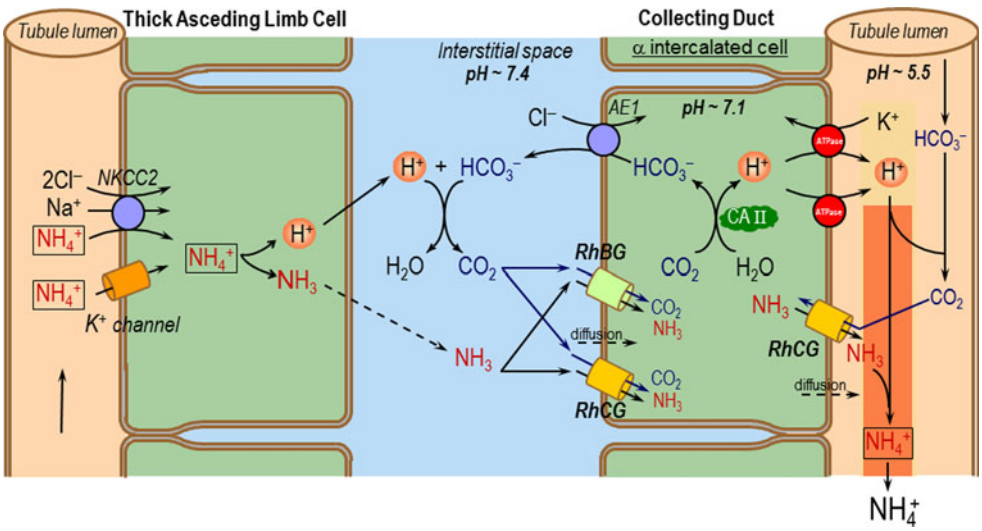

Fig. 8 Proposed novel model for CO_2 and NH_3 transport across the basolateral and apical membranes of αIC cells in the CD. This mechanism, particularly the aspects related to CO_2 movements, is an extension of the models proposed by others (Gruswitz et al. 2010). *Dashed arrows* represent the possible diffusion of CO_2 or NH_3 across plasma membranes. *NKCC2* Na–K–2Cl cotransporter, *AE1* chloride bicarbonate exchanger, *CA II* carbonic anhydrase II

escape into the blood. Moreover, any NH_4^+ that escapes into the blood represents a net loss of urinary NH_3/NH_4^+ that would compromise acid–base balance.

The sustained formation of NH_4^+ in the CD lumen requires not only NH_3 secretion across the apical membrane but also H^+ secretion to titrate the secreted NH_3 to NH_4^+. This secreted H^+ also titrates other luminal buffers, including some HCO_3^-. Regardless of what the secreted H^+ titrates, an equivalent amount of HCO_3^- must exit the cell across the basolateral membrane of the CD cell via the renal form of AE1 (Romero 2005). The source of this cytosolic HCO_3^- is CO_2. The aforementioned models neither implicitly assume that CO_2 can freely enter the CD cell across the basolateral membrane by an unspecified mechanism nor explicitly state that the CO_2 enters by dissolving in the lipid phase of the plasma membrane. We propose that the bifunctional RhBG and RhCG channels in the CD are important not only for mediating NH_3 uptake across the basolateral membrane but also for mediating CO_2 uptake. Moreover, to the extent that the H^+ secreted into the CD lumen titrates a small amount of luminal HCO_3^- to form CO_2, this CO_2 could enter the αIC via apical RhCG. Thus, the RhBG and RhCG would enhance CO_2 uptake into the αIC, thereby speeding luminal H^+ secretion.

Conclusions

Our results confirm the observation that the human rhesus family of transporters—RhAG, RhBG and RhCG—exhibit significant permeability to NH_3 and show for the first time that RhBG and RhCG can conduct CO_2. We could not assess the effect of specific Asp to Asn mutations (equivalent to D160 in AmtB) on the CO_2 and NH_3 permeability of RhBG and RhCG because these mutants have an extremely low abundance in the oocyte plasma membrane. Finally, we could not distinguish the CO_2/NH_3 permeability ratios of RhAG, RhBG and RhCG in this study.

Acknowledgments We thank Dale Huffman for computer support, Dr. Alice Brown (University of Bristol) for plasmid cloning and Dr. Nancy Amaral Rebouças (University of São Paulo) and Dr. Seong-Ki Lee (Case Western Reserve University) for helpful discussions. R. R. G. was supported by postdoctoral fellowship N00014-09-1-0246 from the Office of Naval Research. R. M.-A. was supported by Fundação de Amparo a Pesquisa do Estado de São Paulo (FAPESP, 08/128663). This work was supported by Office of Naval Research grant N00014-11-1-0889 and NIH grant DK81567 to W. F. B. A. M. T. received funding from Kidney Research UK and NHS Blood and Transplant R&D.

References

Attmane-Elakeb A, Amlal H, Bichara M (2001) Ammonium carriers in medullary thick ascending limb. Am J Physiol Renal Physiol 280:F1–F9

Bakouh N, Benjelloun F, Cherif-Zahar B, Planelles G (2006) The challenge of understanding ammonium homeostasis and the role of the Rh glycoproteins. Transfus Clin Biol 13:139–146

Bishop JM, Verlander JW, Lee H-W et al (2010) Role of the rhesus glycoprotein, Rh B glycoprotein, in renal ammonia excretion. Am J Physiol Renal Physiol 299:F1065–F1077

Biver S, Belge H, Bourgeois S et al (2008) A role for rhesus factor Rhcg in renal ammonium excretion and male fertility. Nature 456:339–343

Boron WF, Boulpaep EL (1983) Intracellular pH regulation in the renal proximal tubule of the salamander. Basolateral HCO_3^- transport. J Gen Physiol 81:53–94

Brion LP, Schwartz JH, Zavilowitz BJ, Schwartz GJ (1988) Micromethod for the measurement of carbonic anhydrase activity in cellular homogenates. Anal Biochem 175:289–297

Brown ACN, Hallouane D, Mawby WJ et al (2009) RhCG is the major putative ammonia transporter expressed in the human kidney, and RhBG is not expressed at detectable levels. Am J Physiol Renal Physiol 296:F1279–F1290

Bruce LJ, Guizouarn H, Burton NM et al (2009) The monovalent cation leak in overhydrated stomatocytic red blood cells results from amino acid substitutions in the Rh-associated glycoprotein. Blood 113:1350–1357

Cooper GJ, Boron WF (1998) Effect of pCMBS on CO_2 permeability of *Xenopus* oocytes expressing aquaporin 1 or its C189S mutant. Am J Physiol Cell Physiol 275:C1481–C1486

Eladari D, Cheval L, Quentin F et al (2002) Expression of RhCG, a new putative NH_3/NH_4^+ transporter, along the rat nephron. J Am Soc Nephrol 13:1999–2008

Endeward V, Musa-Aziz R, Cooper GJ et al (2006) Evidence that aquaporin 1 is a major pathway for CO_2 transport across the human erythrocyte membrane. FASEB J 20:1974–1981

Endeward V, Cartron J-P, Ripoche P, Gros G (2008) RhAG protein of the rhesus complex is a CO_2 channel in the human red cell membrane. FASEB J 22:64–73

Geyer RR, Musa-Aziz R, Enkavi G et al (2013a) Movement of NH_3 through the human urea transporter B (UT-B): a new gas channel. Am J Physiol Renal Physiol. doi:10.1152/ajprenal.00609.2012

Geyer RR, Musa-Aziz R, Qin X, Boron WF (2013b) Relative CO_2/NH_3 selectivities of mammalian aquaporins 0–9. Am J Physiol Cell Physiol. doi:10.1152/ajpcell.00033.2013

Giebisch G, Windhager EE (2009) Urine concentration and dilution. In: Boron WF, Boulpaep EL (eds) Medical physiology: a cellular and molecular approach, 2nd edn. Elsevier, Philadelphia, pp 835–850

Gruswitz F, Chaudhary S, Ho JD et al (2010) Function of human Rh based on structure of RhCG at 2.1 Å. Proc Natl Acad Sci USA 107:9638–9643

Han K-H, Croker BP, Clapp WL et al (2006) Expression of the ammonia transporter, Rh C glycoprotein, in normal and neoplastic human kidney. J Am Soc Nephrol 17:2670–2679

Han K-H, Mekala K, Babida V et al (2009) Expression of the gas-transporting proteins, Rh B glycoprotein and Rh C glycoprotein, in the murine lung. Am J Physiol Lung Cell Mol Physiol 297:L153–L163

Han K-H, Lee H-W, Handlogten ME et al (2013) Expression of the ammonia transporter family member, Rh B glycoprotein, in the human kidney. Am J Physiol Renal Physiol 304:F972–F981

Herrera M, Garvin JL (2007) Novel role of AQP-1 in NO-dependent vasorelaxation. Am J Physiol Renal Physiol 292:F1443–F1451

Herrera M, Hong NJ, Garvin JL (2006) Aquaporin-1 transports NO across cell membranes. Hypertension 48:157–164

Javelle A, Severi E, Thornton J, Merrick M (2004) Ammonium sensing in *Escherichia coli*: role of the ammonium transporter AmtB and AmtB-GlnK complex formation. J Biol Chem 279:8530–8538

Kaldenhoff R (2012) Mechanisms underlying CO_2 diffusion in leaves. Curr Opin Plant Biol 15:276–281

Kaldenhoff R, Fischer M (2006) Aquaporins in plants. Acta Physiol (Oxf) 187:169–176

Kim H-Y, Verlander JW, Bishop JM et al (2009) Basolateral expression of the ammonia transporter family member Rh C glycoprotein in the mouse kidney. Am J Physiol Renal Physiol 296:F543–F555

Lee H-W, Verlander JW, Bishop JM et al (2009) Collecting duct-specific Rh C glycoprotein deletion alters basal and acidosis-stimulated renal ammonia excretion. Am J Physiol Renal Physiol 296:F1364–F1375

Lee H-W, Verlander JW, Bishop JM et al (2010) Effect of intercalated cell–specific Rh C glycoprotein deletion on basal and metabolic acidosis–stimulated renal ammonia excretion. Am J Physiol Renal Physiol 299:F369–F379

Lopez C, Métral S, Eladari D et al (2005) The ammonium transporter RhBG: requirement of a tyrosine-based signal and ankyrin-G for basolateral targeting and membrane anchorage in polarized kidney epithelial cells. J Biol Chem 280:8221–8228

Ludewig U (2004) Electroneutral ammonium transport by basolateral rhesus B glycoprotein. J Physiol (Lond) 559:751–759

Mak D-OD, Dang B, Weiner ID et al (2006) Characterization of ammonia transport by the kidney Rh glycoproteins RhBG and RhCG. Am J Physiol Renal Physiol 290:F297–F305

Marini AM, Boeckstaens M, Benjelloun F et al (2006) Structural involvement in substrate recognition of an essential aspartate residue conserved in Mep/Amt and Rh-type ammonium transporters. Curr Genet 49:364–374

Musa-Aziz R, Chen L-M, Pelletier MF, Boron WF (2009a) Relative CO_2/NH_3 selectivities of AQP1, AQP4, AQP5, AmtB, and RhAG. Proc Natl Acad Sci USA 106:5406–5411

Musa-Aziz R, Jiang L, Chen L-M et al (2009b) Concentration-dependent effects on intracellular and surface pH of exposing *Xenopus* oocytes to solutions containing NH_3/NH_4^+. J Membr Biol 228:15–31

Musa-Aziz R, Boron WF, Parker MD (2010) Using fluorometry and ion-sensitive microelectrodes to study the functional expression of heterologously-expressed ion channels and transporters in *Xenopus* oocytes. Methods 51:134–145

Nagami GT (1988) Luminal secretion of ammonia in the mouse proximal tubule perfused in vitro. J Clin Invest 81:159–164

Nakhoul NL, Davis BA, Romero MF, Boron WF (1998) Effect of expressing the water channel aquaporin-1 on the CO_2 permeability of *Xenopus* oocytes. Am J Physiol Cell Physiol 274: C543–C548

Nakhoul NL, Hering-Smith KS, Abdulnour-Nakhoul SM, Hamm LL (2001) Transport of NH_3/NH_4^+ in oocytes expressing aquaporin-1. Am J Physiol Renal Physiol 281:F255–F263

Quentin F, Eladari D, Cheval L et al (2003) RhBG and RhCG, the putative ammonia transporters, are expressed in the same cells in the distal nephron. J Am Soc Nephrol 14:545–554

Ripoche P, Bertrand O, Gane P et al (2004) Human rhesus-associated glycoprotein mediates facilitated transport of NH_3 into red blood cells. Proc Natl Acad Sci USA 101:17222–17227

Ripoche P, Goossens D, Devuyst O et al (2006) Role of RhAG and AQP1 in NH_3 and CO_2 gas transport in red cell ghosts: a stopped-flow analysis. Transfus Clin Biol 13:117–122

Romero MF (2005) Molecular pathophysiology of SLC4 bicarbonate transporters. Curr Opin Nephrol Hypertens 14:495–501

Romero MF, Hediger MA, Boulpaep EL, Boron WF (1997) Expression cloning and characterization of a renal electrogenic $Na^+CO_3^-$ cotransporter. Nature 387:409–413

Seshadri RM, Klein JD, Kozlowski S et al (2006) Renal expression of the ammonia transporters, Rhbg and Rhcg, in response to chronic metabolic acidosis. Am J Physiol Renal Physiol 290:F397–F408

Singh SK, Binder HJ, Geibel JP, Boron WF (1995) An apical permeability barrier to NH_3/NH_4^+ in isolated, perfused colonic crypts. Proc Natl Acad Sci USA 92:11573–11577

Somersalo E, Occhipinti R, Boron WF, Calvetti D (2012) A reaction-diffusion model of CO_2 influx into an oocyte. J Theor Biol 309:185–203

Toye AM, Williamson RC, Khanfar M et al (2008) Band 3 Courcouronnes (Ser667Phe): a trafficking mutant differentially rescued by wild-type band 3 and glycophorin A. Blood 111:5380–5389

Uehlein N, Lovisolo C, Siefritz F, Kaldenhoff R (2003) The tobacco aquaporin NtAQP1 is a membrane CO_2 pore with physiological functions. Nature 425:734–737

Uehlein N, Sperling H, Heckwolf M, Kaldenhoff R (2012) The *Arabidopsis* aquaporin PIP1;2 rules cellular CO_2 uptake. Plant Cell Environ 35:1077–1083

Verlander JW, Miller RT, Frank AE et al (2003) Localization of the ammonium transporter proteins RhBG and RhCG in mouse kidney. Am J Physiol Renal Physiol 284:F323–F337

Wagner CA, Devuyst O, Bourgeois S, Mohebbi N (2009) Regulated acid-base transport in the collecting duct. Pflugers Arch 458:137–156

Wagner CA, Devuyst O, Belge H et al (2011) The rhesus protein RhCG: a new perspective in ammonium transport and distal urinary acidification. Kidney Int 79:154–161

Waisbren SJ, Geibel JP, Modlin IM, Boron WF (1994) Unusual permeability properties of gastric gland cells. Nature 368:332–335

Weiner ID, Verlander JW (2010) Molecular physiology of the Rh ammonia transport proteins. Curr Opin Nephrol Hypertens 19:471–477

Weiner ID, Verlander JW (2011) Role of NH_3/NH_4^+ transporters in renal acid-base transport. Am J Physiol Renal Physiol 300:F11–F23

Zidi-Yahiaoui N, Mouro-Chanteloup I, D'Ambrosio A-M et al (2005) Human rhesus B and rhesus C glycoproteins: properties of facilitated ammonium transport in recombinant kidney cells. Biochem J 391:33–40